

Electronic Supplementary Information

**Scaffolding an Ultrathin CdS Layer on ZnO Nanorods Array using
Pulsed Electrodeposition for Improved Photocharge Transport under
Visible Light Illumination**

Yiming Tang, Patrapark Traveerungroj, Hui Ling Tan, Peng Wang, Rose Amal†, and Yun Hau Ng†

Particles and Catalysis Research Group, School of Chemical Engineering, The University of New South Wales, Sydney NSW 2052, Australia

†Email: r.amal@unsw.edu.au; yh.ng@unsw.edu.au

Supporting Figures

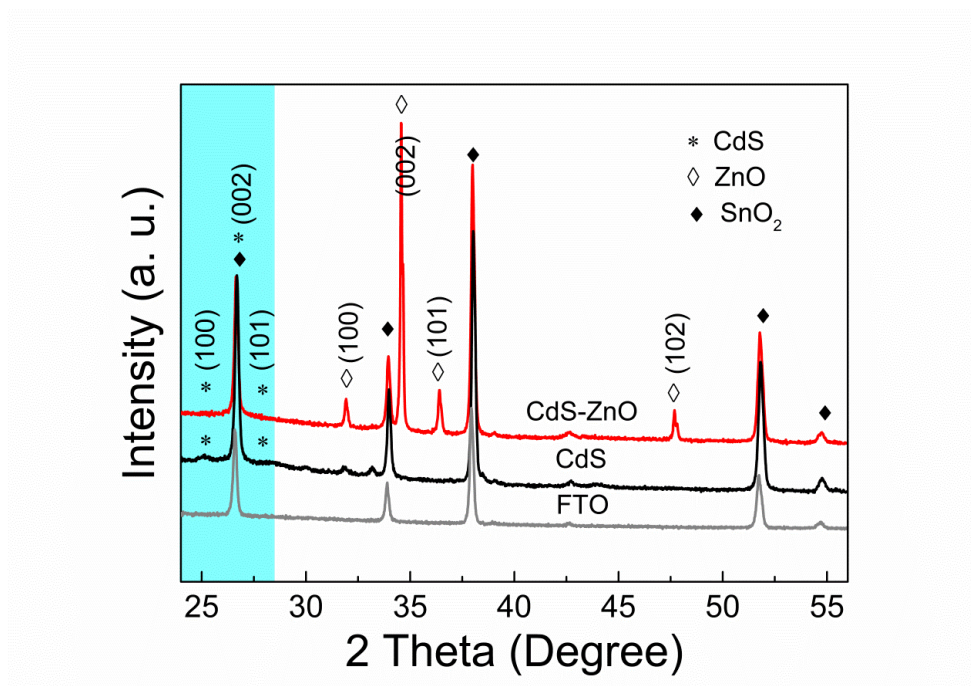


Figure S1. XRD patterns of FTO substrate, CdS film and CdS-ZnO film from pulsed electrodeposition.

Figure S1 shows the XRD patterns of CdS film and CdS-ZnO film using pulsed electrodeposition. In the CdS trace, three typical peaks at 24.86° , 26.45° and 28.22° assigning to the (100), (002) and (101) patterns of CdS have been observed, demonstrating the typical hexagonal structure on the FTO substrate. Note that the characteristic peak of CdS at 26.45° (002) is overlapping with 26.61° (110) from the substrate. The intensities of the CdS characteristic peaks are quite low due to the insufficient amount of CdS. After pulsed electrodeposition on the ZnO nanorods, XRD diffraction peaks at 32° , 34.5° , 36.3° exhibits the typical patterns assigning to hexagonal ZnO nanorods from chemical bath deposition. However the relative low amount of CdS compare to ZnO makes it harder to be detected.

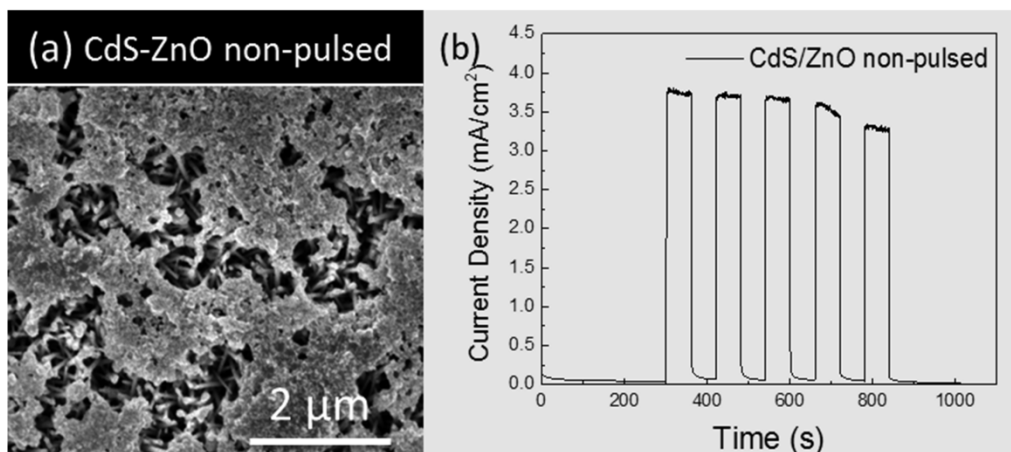


Figure S2. (a) SEM images of CdS-ZnO from non-pulsed electrodeposition (chronoamperometry) for 30 min; (b) PEC measurement of the obtained CdS-ZnO photoelectrode at 0 V vs. Ag/AgCl bias in a three electrode system containing 0.25 M Na₂S and 0.35 M Na₂SO₃ (pH = 12) as the electrolyte under chopped visible light irradiation ($\lambda \geq 435$ nm)

Figure S2a shows the surface morphology of CdS-ZnO composites from non-pulsed electrodeposition of CdS on ZnO nanorod. The duration time and the voltage have adapted to be 30 min and -1.25 V vs. Ag/AgCl. A layer of CdS film with porous structure and aggregated grains was formed on the top of the ZnO nanorod film. Under chronoamperometry condition, the rapid nucleation process due to the continuing current leads to the coalescing of the nuclei.¹ On contrast, the pulsed electrodeposition process of CdS results in more fine-grained CdS and uniform coating on ZnO nanorods. Figure S2b shows the photoelectrochemical property of the obtained composite, yielding an anodic current of approximately 3.3 mA/cm². Therefore in this work we use pulsed electrodeposition to synthesis the well-covered CdS-ZnO electrode.

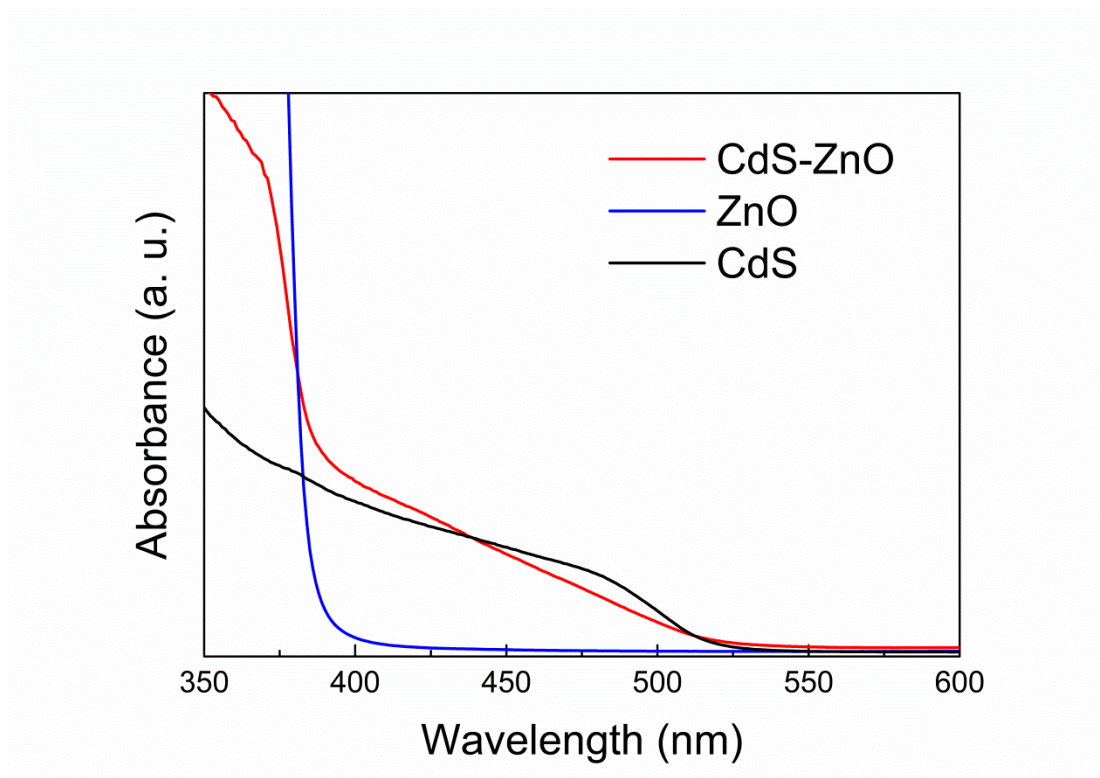


Figure S3. Absorption spectra of pristine ZnO, pure CdS and CdS-ZnO

Figure S3 shows the UV-Vis absorbance spectra of the pristine ZnO nanoarrays, pure CdS and CdS-ZnO composites films. The strong absorbance of the pristine ZnO film starts at approximately 380 nm corresponding to its wide bandgap value of 3.26 eV and has no obvious absorbance within the visible light range. The CdS-ZnO film shows a broad and strong absorbance from approximately 520 nm to the UV region, indicating the effective extension of visible light absorption also reflected by its narrow bandgap of 2.4 eV.

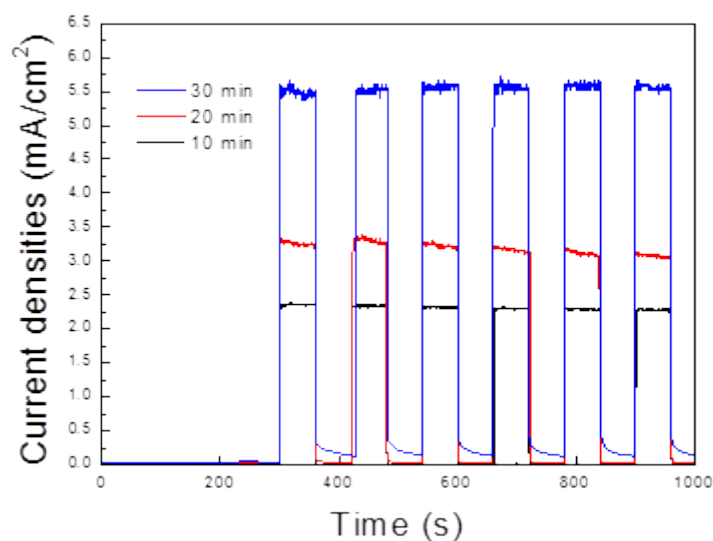


Figure S4 Photoelectrochemical measurement of CdS-ZnO photoelectrodes using different durations 10 min, 20 min and 30 min from pulsed electrodeposition.

The thickness of CdS is crucial in charge separation behaviour as the electron diffusion length of CdS would affect the electron transfer from the surface of the CdS layer to the interface of CdS-ZnO. As the amount of CdS deposit is a function of electrodeposition time, we varied the duration of pulsed electrodeposition from 10 min, 20 min to 30 min as one way to study the effect of CdS thickness on the photocurrent generation. As shown in the figure below, it has been found that with the increase in electrodeposition duration, the photocurrent generated from CdS-ZnO was increased. However, as limited by the diffusion of precursor, a further extended electrodeposition time will result in the blockage of the entrance of the nanorod arrays and thus leading to the decrease of photoactivity.

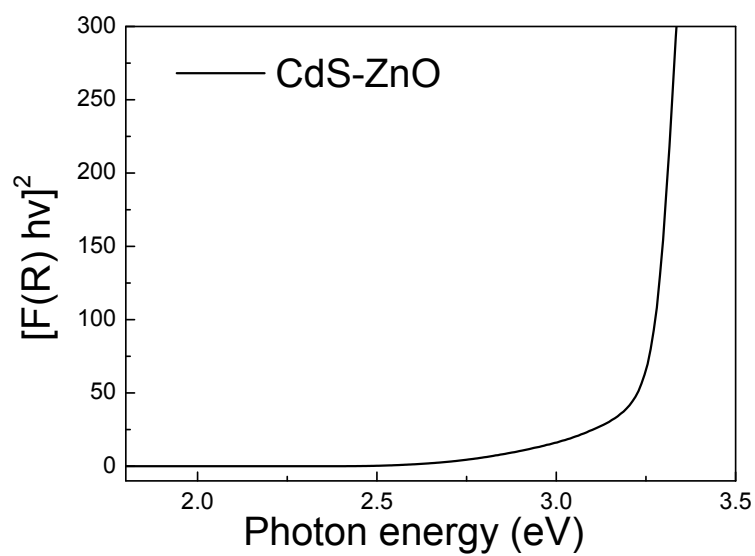


Figure S5. Tauc plot of CdS-ZnO composites

Figure S5 shows the Tauc plot of CdS-ZnO composites. Two absorption bands indicate two components in the composites. The band gaps of the two components are around 2.4 eV and 3.25 eV, which shows great agreement with the bandgap of CdS and ZnO, respectively.

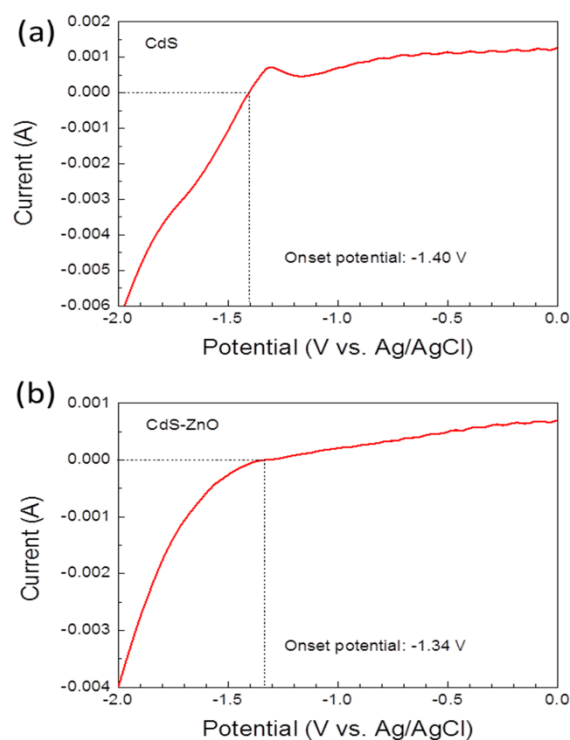


Figure S6. Linear sweep of CdS and CdS-ZnO photoelectrodes in a three-electrode system: a Pt wire as a counter electrode, a Ag/AgCl as a reference electrode and polysulfide solution as the electrolyte) under visible light illumination ($\lambda \geq 435$ nm) from -2.0 V vs. Ag/AgCl to 0 V vs. Ag/AgCl.

Figure S6 shows the linear sweep of CdS and CdS-ZnO photoelectrodes under visible light irradiation. A slightly positive shift of 0.06 V of onset potential has been observed after introducing ZnO between CdS and FTO substrate due to the conduction band alignment of CdS and ZnO from the CdS-ZnO composite.

Reference

- (1) G. Holmbom and B. E. Jacobson, *J. Electrochem. Soc.*, 1988, **135**, 2720.